

ASSESSING NON-NORMAL EFFECTS IN THERMOACOUSTIC SYSTEMS WITH NON ZERO BASELINE FLOW

K. Wieczorek¹, C. Sensiau², W. Polifke³, F. Nicoud*⁴

¹ CFD-Team, CERFACS, 42 Ave Coriolis, 31057 Toulouse, France

² SNECMA Villaroche, France

³ Lehrstuhl für Thermodynamik, TU Munich, 85747 Garching, Germany

⁴ I3M, University Montpellier 2, CC51, 34057 Montpellier Cedex 5, France

* Corresponding author: franck.nicoud@univ-montp2.fr

In this paper, the theory of non-normal interaction is applied to eigenmodes of a thermoacoustic system that include mean flow effects. When the mean flow is taken into account, the energy associated to the eigenmodes contains not only contributions of the acoustic field, but also those of convected entropy and vorticity modes. The notion of maximum transient energy growth is therefore extended from an energy expression based on the classical acoustic energy to a form based on the generalized disturbance energy. The approach is applied to a 1D configuration that consists in a duct including a 1D flame followed by a choked isentropic nozzle. It is shown that for such a case it is essential to include the contribution of entropy perturbations in the calculation of the optimal initial perturbation and the maximum transient energy growth.

1 Introduction

Over the last decades, thermoacoustic instabilities have been the subject of intense research activity with the aim to better understand and eventually predict/avoid them at the design level. Except when the equations are solved in the time domain (e.g. when Large Eddy Simulation is used), the analysis most often relies on a modal approach, where the first eigenmodes/eigenfrequencies of the thermoacoustic system are sought for. Since these modes are not orthogonal in general because of boundary conditions and/or flame coupling [17], the associated frequencies only provide information about the long term evolution of the system, which is linearly stable if and only if all its modes are damped. However, if non-normality is present, linear modes may interact and transient energy growth can be observed even for stable systems. This effect was demonstrated theoretically by Balasubramanian & Sujith [2] who translated ideas initially developed for classical fluid mechanics [13, 22, 26].

The maximum energy growth that can appear depends only on the thermoacoustic system of interest. Calling \mathcal{U} the state vector (typically the components of \mathcal{U} are the fields of acoustic density, pressure and velocity), the relevant equations for describing the time evolution of the perturbations read formally:

$$\frac{\partial \mathcal{U}}{\partial t} + \mathcal{A}(\mathcal{U}) = 0, \quad (1)$$

where \mathcal{A} is a differential operator which is linear when linear thermoacoustics is considered. Eq. (1) is nothing but a set of partial differential equations which can be reduced to a set of ordinary differential equations when an appropriate discretization method is used. The thermoacoustic system of interest is

then represented by a first order dynamical system which reads:

$$\frac{d\mathbf{u}}{dt} + \mathbf{A}\mathbf{u} = 0, \quad (2)$$

where \mathbf{u} is the discretized counterpart of \mathcal{U} . If Eq. (2) is obtained from Eq. (1) using a Galerkin technique, i.e. by expanding the fluctuating quantities as series of orthogonal basis functions [5], the vector \mathbf{u} contains the weights of those basis functions. On the other hand, if a finite difference/finite volume technique is used, \mathbf{u} contains the nodal values of the state vector \mathcal{U} . Of course, the square matrix \mathbf{A} depends on the discretization technique, both in its size and structure. Typically, a Galerkin method produces a dense matrix of small size, as the expansion requires usually only few basis functions (e.g.: [16]). In difference to that, a finite volume approach produces a large but sparse matrix (e.g.: [19]). In any case, some of the characteristics of the thermoacoustic system can be studied by analyzing the matrix \mathbf{A} instead of the differential operator \mathcal{A} . Notably, the maximum transient energy growth at time t , $G(t)$, is related to the largest singular value of the exponential matrix $\exp(-\mathbf{A}t)$ [22]. This property was used in several recent studies in order to quantify the non-normal effects in simple thermoacoustic systems such as the Rijke tube [2] or a laminar diffusion flame [1]. This allowed assessing the maximum transient growth $G_{max} = \max[G(t)]$, the maximum value being taken over all the possible values of t . Unfortunately, we believe that this approach based on a Singular Value Decomposition (SVD) of the matrix \mathbf{A} is not very suitable for complex systems for two main reasons:

1. **time delay:** In practical cases, the flame response to upstream acoustic perturbations is time lagged, the time delay τ being potentially related to several fluid mechanics and/or chemical processes relevant to the flame unsteadiness. In thermo-acoustic simulations based on linearized equations this time lag behaviour has to be included explicitly in the system of equations via the flame model. As a consequence, the system cannot be described by Eq. (1), but an expression of the form

$$\frac{\partial \mathcal{U}}{\partial t} + \mathcal{A}(\mathcal{U}(t)) + \mathcal{B}(\mathcal{U}(t - \tau)) = 0, \quad (3)$$

must be used instead. Unfortunately, generalizing the SVD approach described above to Eq. (3) is not straightforward and may involve additional simplifications like assuming the time delay τ to be small compared to the first mode's period [16].

2. **boundary conditions:** if the Galerkin method is used to degrade Eq. (1) into Eq. (2), the knowledge of an orthogonal set of basis functions which meet the actual boundary conditions of the thermoacoustic problem is required. Because they convey useful information about the configuration, the acoustic eigenmodes are good candidates (e.g.: [5]) for this purpose. Unfortunately, they are not orthogonal as soon as the boundary conditions correspond to a finite, complex valued impedance [17], a situation which is not rare. If a finite difference/finite volume type of approach is used instead for degrading Eq. (1), the size of the discretized problem, Eq. (2), is large (typical finite volume grids contain $10^5 - 10^6$ elements) so that performing a SVD in order to assess $G(t)$ may be CPU demanding. Thus, maximizing $G(t)$ over all the values of time t to obtain G_{max} might not be affordable in practice.

Recently, Selimefendigil et al. [23] proposed a method to handle delayed systems and overcome the first issue mentioned. In their view, Eq. (3) is recast into an equivalent non-delayed problem for which the pseudospectra can be computed. The concept of pseudospectra (first mentioned by Landau [11]) was introduced by Trefethen [25] in order to quantify the sensitivity of eigenvalues to uncertainties/ perturbations in the data or discretization. The property exploited by Selimefendigil et al. [23] is that the geometry of pseudospectra can be used to obtain a lower bound of G_{max} (Kreiss theorem). Still, computing pseudospectra becomes very CPU demanding when the size of the problem increases so that this approach does not address the second issue mentioned. Besides, as far as the authors know, analyzing the pseudospectra can only give information about the maximum transient growth and not about the shape of the optimal perturbation.

The first objective of this paper is to assess a strategy which is potentially suitable for assessing non-normal effects in 3D complex configurations and not CPU demanding. It relies heavily on the knowl-

edge of the first few thermoacoustic eigenmodes of the system of interest. Indeed, even if non-normality is present and eigenmodes only provide information about the long term evolution, they convey relevant information about the system. For example, their individual stability dictates the overall stability of the system if non-linear effects are not considered. Numerical strategies have been proposed in the past in order to compute such modes by solving an Helmholtz type of equation with a forcing term representing the flame [9, 17, 24]. The view considered in this paper was initially proposed by Schmid & Henningson [22] for investigating classical fluid mechanics configurations. It consists in looking for the optimal perturbation (the one which generates the largest transient growth) in the linear space spanned by the thermoacoustics modes. In other words, assessing the non-normality effect appears as a post-processing of the results of the classical modal characterization of the configuration. As we will demonstrate, this is virtually done at no additional cost. Of course, since only a finite number of eigenmodes are considered, all the possible perturbations cannot be generated by combining these modes and only a lower bound of G_{\max} can be obtained. However, since the eigenmodes convey a lot of information regarding the system of interest, it is expected that keeping only a few of them is sufficient to obtain a reasonable assessment of the maximum transient growth. The same idea justifies the Galerkin methods where often only a few (of order 10 say) basis functions are necessary to reach good accuracy. However, contrary to the Galerkin method, the orthogonality of the modes is not required in the present approach so that the method is also suitable for complex 3D configurations with finite valued boundary impedance.

All the previous studies dealing with non-normal effects in thermoacoustic systems relied on the zero mean flow assumption although the effect of the approximation $M \simeq 0$ is not well understood [6] and the neglected convective terms may introduce additional non-normality [7]. In the case of a premixed 1D flame, only a moderate non-normal effect was found in the literature [2], the maximum transient energy growth (G_{\max}) being close to 7. The second objective of this paper is then to investigate if larger values of G_{\max} can be observed when the baseline flow is not assumed at rest. In this case, the evolution of the perturbations are described by the Linearized Euler Equations instead of a simple Helmholtz equation for the acoustic pressure. Also, the state vector contains one more component (the density or entropy say) on top of the acoustic pressure and velocity fields. Thus this situation is quite different from what has been considered so far in the literature and the presented analysis also serves as an illustration of the flexibility of the method and its ability to handle complex situations.

The formalism of the method is detailed in sections 2.2 and 2.3 in the case of a generic 3D thermoacoustic system written under the zero Mach number assumption and described in section 2.1. In this case, the state vector contains only the acoustic pressure and velocity fields and non-trivial boundary conditions (finite, complex valued impedance) can be considered. The formalism is then extended in section 2.4 to the case where the perturbations are obtained from the LEE and the state vector contains one more component. The method is then illustrated by analyzing the simple case of a 1D flame stabilized within a straight duct. Note however that this situation is more complex than several previous studies since **a**) a time delayed $n\text{-}\tau$ type of model is used for describing the acoustic-flame coupling and **b**) complex boundary conditions are applied at the boundaries of the duct. The corresponding results are discussed in section 3 where the maximum transient growth related to two types of energies is considered, i.e. the classical acoustic energy and the energy of the fluctuations.

2 Formalism

2.1 The thermoacoustic model

The phenomenon of thermoacoustic instability results from a coupling between combustion processes and the acoustic eigenmodes of the configuration (among many others: [12]). Assuming vanishing Mach number for the mean flow, this coupling can be modeled in the linear regime by the following wave equation :

$$\frac{1}{\gamma(\mathbf{x})p_0} \frac{\partial^2 p'(\mathbf{x}, t)}{\partial t^2} + \nabla \cdot \frac{1}{\rho_0(\mathbf{x})} \vec{\nabla} p'(\mathbf{x}, t) = \frac{\gamma(\mathbf{x}) - 1}{\gamma(\mathbf{x})p_0} \frac{\partial q'(\mathbf{x}, t)}{\partial t}, \quad (4)$$

where $p'(\mathbf{x}, t)$ stands for the acoustic pressure at position \mathbf{x} and time t ; $\gamma(\mathbf{x})$ and $\rho_0(\mathbf{x})$ are the time averaged isentropic coefficient and density of the fluid; p_0 is the homogeneous background pressure. Eq. (4) states that heat release fluctuations $q'(\mathbf{x}, t)$ may influence the acoustics in the domain. It is common practice to model the feedback effect, viz. the influence of acoustic fluctuations on combustion, via an $n - \tau$ type of model [3, 4, 21]. This model assumes that the heat release fluctuations are proportional to the time-lagged velocity fluctuations at a reference point located upstream of the flame:

$$q'(\vec{x}, t) = \frac{q_{tot}}{u_{bulk}} H_q(\mathbf{x}) \mathbf{u}'(\mathbf{x}_{ref}, t - \tau) \cdot \mathbf{n}_{ref}, \quad (5)$$

where $H_q(\mathbf{x})$ is the amplitude of the flame response and can be related to the parameter n of $n - \tau$ models [19], $\tau(\mathbf{x})$ is the time delay and \mathbf{n}_{ref} is a unit vector. Assuming time-harmonic perturbations of pulsation ω , one may write $p'(\mathbf{x}, t) = \Re(\hat{p}(\mathbf{x})e^{-i\omega t})$ and $q'(\vec{x}, t) = \Re(\hat{q}(\mathbf{x})e^{-i\omega t})$. The acoustic field can then be expressed in terms of eigenmodes that are solution of a Helmholtz equation written for the complex amplitude of pressure \hat{p} :

$$\gamma(\mathbf{x})p_0\nabla \cdot \left(\frac{1}{\rho_0(\mathbf{x})} \vec{\nabla} \hat{p}(\mathbf{x}) \right) + \omega^2 \hat{p}(\mathbf{x}) = \frac{q_{tot}}{i\omega\rho_{ref}u_{bulk}} H_q(\mathbf{x}) e^{i\omega\tau(\mathbf{x})} \vec{\nabla} \hat{p}(\mathbf{x}_{ref}) \cdot \mathbf{n}_{ref} \quad (6)$$

As the problem has been written in frequency domain, the reflection of low frequency waves at the boundaries can be handled easily with a complex valued impedance at the boundary, noted Z . The appropriate boundary condition to impose to \hat{p} takes the following form:

$$\vec{\nabla} \hat{p}(\mathbf{x}) \cdot \mathbf{n}_{BC} - i \frac{\omega}{c_0(\mathbf{x})Z(\omega)} \hat{p}(\mathbf{x}) = 0, \quad (7)$$

where \mathbf{n}_{BC} is a unit vector normal to the boundary and $c_0(\mathbf{x})$ is the speed of sound. Solving the eigenproblem given by Eq. (6) and Eq. (7) allows to determine the thermoacoustic pressure eigenmodes $\hat{p}(\mathbf{x})$, and their corresponding eigenfrequencies ω . The velocity eigenmodes $\hat{\mathbf{u}}(\mathbf{x})$ can then be deduced using the linearised Euler equation written in the frequency domain for time harmonic fluctuations:

$$i\omega\rho_0 \hat{\mathbf{u}}(\mathbf{x}) = \vec{\nabla} \hat{p}(\mathbf{x}). \quad (8)$$

2.2 Non-orthogonality of the eigenfunction

Non-normality arises from the fact that the thermoacoustic eigenmodes are not orthogonal. Thus, it is important to specify how orthogonality is defined or, equivalently, what is the appropriate inner product. The formalism used throughout this paper is therefore stated in the following.

An acoustic perturbation is defined as a vector composed of pressure and velocity fluctuations p' and \mathbf{u}' that are assumed to be harmonic in time. This allows to write:

$$v'(\mathbf{x}, t) = \begin{bmatrix} p'(\mathbf{x}, t) \\ \mathbf{u}'(\mathbf{x}, t) \end{bmatrix} = \begin{bmatrix} \Re(\hat{p}(\mathbf{x})e^{-i\omega t}) \\ \Re(\hat{\mathbf{u}}(\mathbf{x})e^{-i\omega t}) \end{bmatrix} = \Re(\hat{v}(\mathbf{x})e^{-i\omega t}) \quad (9)$$

where the vector $\hat{v}(\mathbf{x})$ contains the complex amplitudes of pressure and velocity fluctuations, this latter being composed of three components $\hat{\mathbf{u}}(\mathbf{x}) = (\hat{u}_x(\mathbf{x}), \hat{u}_y(\mathbf{x}), \hat{u}_z(\mathbf{x}))$ and $\omega = \omega_r + i\omega_i$ is a complex frequency.

The following considerations are set in the complex space, i.e. the return to a real valued vector is dropped. The solutions of the thermoacoustic system are considered in the form of complex valued vectors

$$v(\mathbf{x}, t) = \hat{v}(\mathbf{x})e^{-i\omega t} = \hat{v}(\mathbf{x})e^{-i\omega_r t} e^{\omega_i t} \quad \text{with} \quad \hat{v}(\mathbf{x}) = \begin{bmatrix} \hat{p}(\mathbf{x}) \\ \hat{\mathbf{u}}(\mathbf{x}) \end{bmatrix} = \begin{bmatrix} \hat{p}(\mathbf{x}) \\ \hat{u}_x(\mathbf{x}) \\ \hat{u}_y(\mathbf{x}) \\ \hat{u}_z(\mathbf{x}) \end{bmatrix} \quad (10)$$

a complex eigenvector.

Considering $v_1(\mathbf{x}, t)$ and $v_2(\mathbf{x}, t)$ two complex vectors that are solution of Eqs. (6), (7) and (8), a weighted

inner product can be defined as follows:

$$\langle v_1(\mathbf{x}, t) | v_2(\mathbf{x}, t) \rangle_W = \int_V (v_1(\mathbf{x}, t)^H W v_2(\mathbf{x}, t)) dV \quad (11)$$

with $v_1(\mathbf{x}, t)^H = \hat{v}(\mathbf{x})^H e^{i\omega_r t} e^{\omega_i t}$ the conjugate transpose of $v_1(\mathbf{x}, t)$, V the volume of the domain that is considered and W a weight matrix.

If W is the identity matrix I , the inner product defined in Eq. (11) applied to an eigenvector $\hat{v}(\mathbf{x})$ yields simply its L_2 -norm:

$$\langle \hat{v}(\mathbf{x}) | \hat{v}(\mathbf{x}) \rangle_I = \int_V \hat{v}^H(\mathbf{x}) I \hat{v}(\mathbf{x}) dV = \|\hat{v}(\mathbf{x})\|_2^2$$

By defining the matrix W in an appropriate way, the product of Eq. (11) can be linked to an equivalent of the acoustic energy associated to the mode $v(\mathbf{x}) = \hat{v}(\mathbf{x})e^{-i\omega t}$. For an eigenvector $\hat{v}(\mathbf{x})$ as defined in Eq. (10), a weight matrix

$$W_{ac} = \begin{pmatrix} \frac{1}{2\gamma p_0(\mathbf{x})} & \frac{u_{0x}}{2c_0^2} & \frac{u_{0y}}{2c_0^2} & \frac{u_{0z}}{2c_0^2} \\ \frac{u_{0x}}{2c_0^2} & \frac{\rho_0(\mathbf{x})}{2} & 0 & 0 \\ \frac{u_{0y}}{2c_0^2} & 0 & \frac{\rho_0(\mathbf{x})}{2} & 0 \\ \frac{u_{0z}}{2c_0^2} & 0 & 0 & \frac{\rho_0(\mathbf{x})}{2} \end{pmatrix} \quad (12)$$

allows to define an equivalent acoustic energy of the form:

$$\begin{aligned} E_{ac}(t) &= \langle v(\mathbf{x}, t) | v(\mathbf{x}, t) \rangle_{W_{ac}} \\ &= \int_V \left(\hat{v}(\mathbf{x})^H e^{i\omega_r t} e^{\omega_i t} W_{ac} \hat{v}(\mathbf{x}) e^{-i\omega_r t} e^{\omega_i t} \right) dV \\ &= e^{2\omega_i t} \int_V \left(\frac{1}{2\gamma p_0(\mathbf{x})} |\hat{p}(\mathbf{x})|^2 + \frac{\rho_0(\mathbf{x})}{2} |\hat{\mathbf{u}}(\mathbf{x})|^2 + \frac{|\hat{p}(\mathbf{x})|}{c_0(\mathbf{x})^2} |\mathbf{u}_0(\mathbf{x}) \cdot \hat{\mathbf{u}}(\mathbf{x})| \right) dV \end{aligned} \quad (13)$$

The term $E_{ac}(t)$ is a real valued energy that is defined based on complex quantities. It shares the same coefficients as the classical acoustic energy. Still, it differs from the latter in the sense that the classical acoustic energy is based on the real parts of the complex signals and will hence be noted $E_{ac,\Re}(t)$ in the following:

$$E_{ac,\Re}(t) = \int_V \left(\frac{1}{2\gamma p_0(\mathbf{x})} p'(\mathbf{x}, t)^2 + \frac{\rho_0(\mathbf{x})}{2} \mathbf{u}'(\mathbf{x}, t)^2 + \frac{p'(\mathbf{x}, t)}{c_0(\mathbf{x}, t)^2} \mathbf{u}_0(\mathbf{x}) \cdot \mathbf{u}'(\mathbf{x}, t) \right) dV \quad (14)$$

The orthogonality of the eigenmodes can now be discussed using the inner product introduced in Eq. (11) together with the weight matrix of Eq. (12). The projection of $\hat{v}_1(\mathbf{x})$ onto $\hat{v}_2(\mathbf{x})$ can be expressed analytically and leads (after some algebra) to the following equation:

$$\langle \hat{v}_1 | \hat{v}_2 \rangle_{W_{ac}} = \frac{1}{2} \frac{1}{\omega_1 - \omega_2^*} \left[\int_S \frac{1}{\rho_0} \left(\hat{p}_1 \frac{\vec{\nabla} \hat{p}_2^*}{\omega_2^*} - \hat{p}_2^* \frac{\vec{\nabla} \hat{p}_1}{\omega_1} \right) dS + i \int_V \frac{\gamma - 1}{\gamma p_0} (\hat{p}_1 \hat{q}_2^* + \hat{p}_2^* \hat{q}) dV \right], \quad (15)$$

where S and V denote the surface and the volume of the domain and $*$ stands for complex conjugates. (The dependency of the complex variables on \mathbf{x} is omitted for clarity, and the mean flow speed is neglected.)

The expression of Eq. (15) is an extension of the result by Nicoud et al. [17], who were considering only pressure fluctuations in their analysis of the eigenmodes' orthogonality, instead of the complete mode structure composed of pressure and velocity terms. Eq. (15) shows that two eigenmodes \hat{v}_1 and \hat{v}_2 are orthogonal when a) boundary impedances are trivial, i.e. they correspond to pressure or velocity nodes with $\hat{p} = 0$ or $\vec{\nabla} \hat{p} = 0$ respectively; and b) no heat release fluctuations occur ($\hat{q} = 0$). However the conditions for orthogonality will most probably never be met in an actual experimental setup, so that non-normality should be considered as the rule for practical thermoacoustic systems.

As a consequence, even if all the eigenmodes are found stable ($\omega_i < 0$) there is a possibility for the equiv-

alent acoustic energy of Eq. (13) to exhibit a transient growth before it eventually vanishes as predicted by the linear modal analysis. The amplitude of the acoustic fluctuations may become significant during this transient phase and the linear assumption is possibly not valid anymore. In particular, it has been shown [20] that gain and phase of the flame transfer function may depend significantly on the amplitude of the velocity fluctuations. This is the reason why non-normality is sometimes related to complex effects such as non-linear triggering [2].

The focus of the present study is however limited to the assessment of non-normality effects in complex configurations and non-linearity is not considered.

2.3 The maximum possible amplification

For complex time-dependant signals of pressure and velocity $q(\mathbf{x}, t)$, a maximum possible amplification $G_{ac}(t)$ can be defined as

$$G_{ac}(t) = \max \frac{E_{ac}(t)}{E_{ac}(0)} = \max_{q(\mathbf{x},0) \neq 0} \frac{\langle q(\mathbf{x}, t) | q(\mathbf{x}, t) \rangle_{W_{ac}}}{\langle q(\mathbf{x}, 0) | q(\mathbf{x}, 0) \rangle_{W_{ac}}} \quad (16)$$

This quantity should be thought of as the upper bound of the envelop of the equivalent acoustic energy. Starting from any perturbation with a unit energy norm, the equivalent acoustic energy term will always remain smaller than or equal to this coefficient: $E_{ac}(t) < G_{ac}(t)$, $\forall t$. Still, there is no reason why the optimal perturbation, which maximizes E_{ac} at time t_1 , should also maximize E_{ac} at time $t_2 \neq t_1$, thus the envelop.

Schmidt & Henningson [22] provide a procedure to assess this maximum possible amplification for complex signals $q(\mathbf{x}, t)$ that can be expressed as a linear combination of m complex eigenmodes:

$$q(\mathbf{x}, t) = \sum_{j=1}^m k_j \hat{v}_j(\mathbf{x}) e^{-i\omega_j t} \quad (17)$$

This expansion of $q(\mathbf{x}, t)$ as a linear combination of eigenmodes can be rewritten in a compact matrix notation as

$$q(\mathbf{x}, t) = \hat{V}(\mathbf{x}) e^{-i\Omega t} \mathbf{k} \quad (18)$$

where the j^{th} column of the matrix $\hat{V}(\mathbf{x})$ contains the complex valued eigenvector $\hat{v}_j(\mathbf{x})$, the diagonal matrix $\Omega = \text{diag}(\omega_1, \omega_2, \dots, \omega_m)$ contains the complex frequencies of the m eigenvectors used for the expansion and the vector \mathbf{k} stores the coefficients k_j of the linear combination Eq. (17).

Introducing Eq. (18) into the definition of the equivalent acoustic energy of Eq. (13), one obtains:

$$\begin{aligned} E_{ac}^m(t) &= \langle q(\mathbf{x}, t) | q(\mathbf{x}, t) \rangle_{W_{ac}} \\ &= \int_V q(\mathbf{x}, t)^H W_{ac} q(\mathbf{x}, t) dV \\ &= \int_V (e^{-i\Omega t} \mathbf{k})^H \hat{V}(\mathbf{x})^H W_{ac} \hat{V}(\mathbf{x}) e^{-i\Omega t} \mathbf{k} dV \\ &= (e^{-i\Omega t} \mathbf{k})^H M_{ac} (e^{-i\Omega t} \mathbf{k}) \end{aligned} \quad (19)$$

where the matrix M contains the inner products of the m selected eigenvectors:

$$M_{ac} = \int_V (\hat{V}(\mathbf{x})^H W_{ac} \hat{V}(\mathbf{x})) dV = \langle \hat{V}(\mathbf{x}) | \hat{V}(\mathbf{x}) \rangle_{W_{ac}} \quad (20)$$

The element kl of this matrix reads:

$$M_{ac}^{kl} = \int_V (\hat{v}_k(\mathbf{x})^H W_{ac} \hat{v}_l(\mathbf{x})) dV \quad (21)$$

Since $\langle \cdot | \cdot \rangle_{W_{ac}}$ is an inner product, M_{ac} is a positive Hermitian matrix so that its Cholesky decomposition exists and yields the square matrix F_{ac} of size m such that $F_{ac}^H F_{ac} = M_{ac}$. Introducing the decomposition of M_{ac} into the acoustic energy term of Eq. (19) one obtains:

$$E_{ac}^m(t) = (F_{ac} e^{-i\Omega t} \mathbf{k})^H (F_{ac} e^{-i\Omega t} \mathbf{k}) \quad (22)$$

This equation shows that $E_{ac}(t)$ is nothing but the L_2 -norm of the vector $F_{ac} e^{-i\Omega t} \mathbf{k}$. Note that in difference to the energy term defined for one single mode (Eq. (13)), the equivalent acoustic energy term for a superposition of several modes is function not only of ω_i , but also of ω_r (via the matrix Ω).

Finally, noting that the Cholesky factor F_{ac} is not singular, the maximum possible amplification at time t takes the following form:

$$G_{ac}^m(t) = \max \frac{E_{ac}^m(t)}{E_{ac}^m(0)} = \max \frac{\|F_{ac} e^{-i\Omega t} \mathbf{k}\|_2^2}{\|F_{ac} \mathbf{k}\|_2^2} = \max_{F_{ac} \mathbf{k}} \frac{\|F_{ac} e^{-i\Omega t} F_{ac}^{-1} F_{ac} \mathbf{k}\|_2^2}{\|F_{ac} \mathbf{k}\|_2^2} \quad (23)$$

By definition, this quantity is the L_2 -norm of the operator $F_{ac} e^{-i\Omega t} F_{ac}^{-1}$. In other words, the maximum amplification at time t is given by the largest singular value of $F_{ac} e^{-i\Omega t} F_{ac}^{-1}$. The optimal initial perturbation is given by the corresponding right singular vector of $F_{ac} e^{-i\Omega t} F_{ac}^{-1}$.

On the LHS of Eq. (23), the superscript m indicates that this expression gives the maximum energy amplification at time t for all the perturbations which can be obtained by combining the m selected eigenvectors (this notation is sufficient if one assumes that the m vectors selected correspond to the m lowest eigenfrequencies). In the same way, the maximum transient growth, which can be obtained by combining these m eigenvectors, can be obtained by maximizing $G_{ac}^m(t)$ over time and shall be noted:

$$G_{max,ac}^m = \max_t G_{ac}^m(t). \quad (24)$$

In the case where the eigenmodes are orthogonal and all damped, the matrices M_{ac} and F_{ac} are both diagonal. Then, Eq. (23) shows that the maximum growth rate equals unity (because $F_{ac} e^{-i\Omega t} F_{ac}^{-1}$ reduces to $e^{-i\Omega t}$) as it is expected when non-normality is not present. As a last comment, we stress the fact that the singular value decomposition is performed on a matrix of size m (which is the number of eigenmodes used to generate the signal), making the above approach computationally inexpensive.

2.4 Extension to non isentropic modes

When the LEE equations are solved instead of the Helmholtz equation for pressure only, the thermoacoustic modes contain one more component, in the presented case the fluctuating entropy. Any mode can thus be represented with the following compact notation :

$$v(\mathbf{x}, t) = \hat{v}(\mathbf{x}) e^{-i\omega t} = \hat{v}(\mathbf{x}) e^{-i\omega_r t} e^{\omega_i t} \quad \text{with} \quad \hat{v}(\mathbf{x}) = \begin{bmatrix} \hat{p}(\mathbf{x}) \\ \hat{\mathbf{u}}(\mathbf{x}) \\ \hat{s}(\mathbf{x}) \end{bmatrix} = \begin{bmatrix} \hat{p}(\mathbf{x}) \\ \hat{u}_x(\mathbf{x}) \\ \hat{u}_y(\mathbf{x}) \\ \hat{u}_z(\mathbf{x}) \\ \hat{s}(\mathbf{x}) \end{bmatrix} \quad (25)$$

To describe the energy contained in this kind of modes, the corollary for disturbance energy derived by Myers [15] and extended by Karimi et al. [10] is appropriate. Thus, instead of the classical acoustic energy of Eq. (14), the following term should be used to determine the total energy of the disturbances:

$$E_{tot,\Re} = \int_V \left(\frac{1}{2\gamma(\mathbf{x}) p_0} p'(\mathbf{x}, t)^2 + \frac{\rho_0(\mathbf{x})}{2} \mathbf{u}'(\mathbf{x}, t)^2 + \frac{\rho_0(\mathbf{x}) T_0(\mathbf{x})}{2C_p(\mathbf{x})} s'(\mathbf{x}, t)^2 + \rho'(\mathbf{x}, t) \mathbf{u}_0(\mathbf{x}) \cdot \mathbf{u}'(\mathbf{x}, t) \right) dV \quad (26)$$

The weight matrix W_{tot} that relates the inner product of Eq. (11) to a complex based equivalent of the total disturbance energy of Eq. (26) reads

$$W_{tot} = \begin{pmatrix} \frac{1}{2\gamma\rho_0} & \frac{u_{0x}}{2c_0^2} & \frac{u_{0y}}{2c_0^2} & \frac{u_{0z}}{2c_0^2} & 0 \\ \frac{u_{0x}}{2c_0^2} & \frac{\rho_0}{2} & 0 & 0 & -\frac{\rho_0 u_{0x}}{2C_p} \\ \frac{u_{0y}}{2c_0^2} & 0 & \frac{\rho_0}{2} & 0 & -\frac{\rho_0 u_{0y}}{2C_p} \\ \frac{u_{0z}}{2c_0^2} & 0 & 0 & \frac{\rho_0}{2} & -\frac{\rho_0 u_{0z}}{2C_p} \\ 0 & -\frac{\rho_0 u_{0x}}{2C_p} & -\frac{\rho_0 u_{0y}}{2C_p} & -\frac{\rho_0 u_{0z}}{2C_p} & \frac{\rho_0 T_0}{2C_p} \end{pmatrix} \quad (27)$$

The resulting energy term reads then

$$\begin{aligned} E_{tot}(t) &= \left\langle v(\mathbf{x}, t) \middle| v(\mathbf{x}, t) \right\rangle_{W_{tot}} \\ &= e^{2\omega_i t} \int_V \left(\frac{1}{2\gamma\rho_0} |\hat{p}|^2 + \frac{\rho_0}{2} |\hat{\mathbf{u}}|^2 + \frac{\rho_0 T_0}{2C_p} |\hat{s}|^2 + \left(\frac{\hat{p}}{c_0^2} - \frac{\rho_0}{C_p} \hat{s} \right) |\mathbf{u}_0 \cdot \hat{\mathbf{u}}| \right) dV \end{aligned} \quad (28)$$

where the dependencies on \mathbf{x} were omitted for clarity.

The energy term based on complex quantities (Eq. (28)) is formally equivalent to the one based on real valued quantities (Eq. (26)), as the last term of the RHS integral can be rewritten using the linearized state equation

$$\hat{p} = \frac{\hat{p}}{c_0^2} - \frac{\rho_0}{C_p} \hat{s}.$$

It can be shown [8] that the matrix W_{tot} defined in Eq. (27) is definite positive as long as the local mean flow Mach number is smaller than a critical value, more precisely if $Ma = \sqrt{\mathbf{u}_0 \cdot \mathbf{u}_0}/c_0 < 1/\gamma$. Since this condition is well satisfied for practical combustion systems, the following integral:

$$\left\langle \hat{v}_1(\mathbf{x}) \middle| \hat{v}_2(\mathbf{x}) \right\rangle_{W_{tot}} = \int_V (\hat{v}_1(\mathbf{x})^H W_{tot} \hat{v}_2(\mathbf{x})) dV \quad (29)$$

defines an inner product. Thus, the analytical development described in section 2.3 remains valid in the non-isentropic case and the maximum growth at time t can be written as:

$$G_{tot}^m(t) = \max_{F_{tot}\mathbf{k}} \frac{E_{tot}^m(t)}{E_{tot}^m(0)} = \max_{F_{tot}\mathbf{k}} \frac{\|F_{tot} e^{-i\Omega t} F_{tot}^{-1} F_{tot}\mathbf{k}\|_2^2}{\|F_{tot}\mathbf{k}\|_2^2} = \|F_{tot} e^{-i\Omega t} F_{tot}^{-1}\|_2^2 \quad (30)$$

where the Cholesky factorisation of the matrix

$$M_{tot} = \int_V (\hat{V}(\mathbf{x})^H W_{tot} \hat{V}(\mathbf{x})) dV = F_{tot}^H F_{tot}$$

has been introduced. This decomposition obviously exists when W_{tot} is symmetric positive definite, i.e. when $Ma < 1/\gamma$ [8]. It might also exist even if the latter condition is not met locally, in a choked nozzle say, where the local mean Mach number is obviously greater than the critical value. This is due to the volume integral in the definition of M_{tot} , which allows some compensation between low and large Mach number regions. Similarly to the isentropic case of section 2.3, the maximum energy at time t is given by the largest singular value of $F_{tot} e^{-i\Omega t} F_{tot}^{-1}$ and the corresponding initial perturbation is given by the right principal singular vector. Besides, the maximum transient growth which can be obtained by combining m eigenvectors is:

$$G_{max,tot}^m = \max_t G_{tot}^m(t). \quad (31)$$

As in the isentropic case of section 2.3, we may remark that :

- Eq. (30) produces $G_{max,tot}^m = 1$ when the eigenmodes are orthogonal and damped,
- the requested singular value decomposition is still to be made on a matrix of size m , thus not very computationally demanding

The theoretical results established in sections 2.3 and 2.4 are now used to study an academic configuration where Mach number effects are present.

3 Results

3.1 Configuration

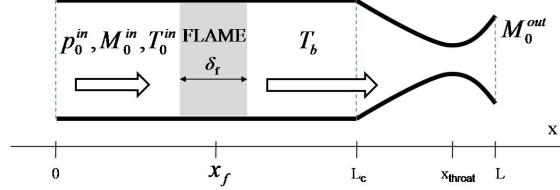


Figure 1: The numerical setup to assess non-normality with non-zero mean flow (from Nicoud and Wieczorek [19]).

L (m)	L_c (m)	x_{throat} (m)	x_f (m)	δ_f (m)	γ	r (S.I)
1.1	1.0	1.0863	0.5	0.15	1.4	287
p_0^{in} (Pa)	$T_0^{\text{in}} = T_u$ (K)	T_b (K)	M_0^{in}	M_0^{out}	x_{ref} (m)	
101325	300	1200	0.05	1.5	0.42	

Table 1: Main physical parameters used for configuration of Fig. 1.

The numerical setup consists in a constant cross section duct of length L_c with a 1D flame of characteristic thickness δ_f located at $x = x_f$ and connected to a nozzle of length $L - L_c$ (see Fig. 1). The mean flow is assumed isentropic except in the flame region and is constructed from analytical expressions of the temperature profile in the combustion chamber and the Mach number distribution in the isentropic nozzle (see Eqs. (4.3) and (4.1) in [19]). The mean flow is then entirely determined by the choice of three independent inlet quantities (for example p_0^{in} , T_0^{in} , M_0^{in}), the outlet Mach number M_0^{out} and relevant geometrical parameters δ_f , x_f , L_c , x_{throat} and L .

The mean profiles depicted in Fig. 2 correspond to the numerical values gathered in Table 1 and used throughout the course of this study. T_u and T_b are the temperature of unburnt and burnt gas respectively. Note that in the presented case, the gain of the flame transfer function H_q of Eq. (5) is set to zero, i.e. unsteady heat release is not considered. However, there is still interaction of the acoustic field with the heat source, as acoustic perturbations generate entropy waves in the flame zone, which are then convected downstream and may in turn create acoustic waves in the nozzle.

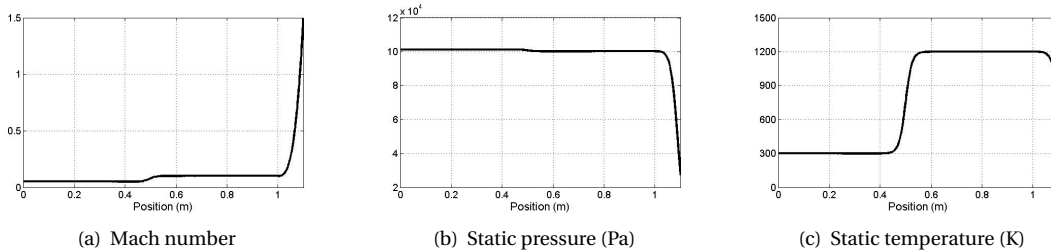


Figure 2: Mean flow fields for the configuration of Fig. 1.

The first eigenmodes of the configuration are computed following the procedure described in [19] where the Linearized Euler Equations written in the frequency space are discretized on a staggered

mesh. The first three modes are displayed in Fig. 3 where the modulus of the complex amplitudes of pressure, velocity and entropy are plotted.

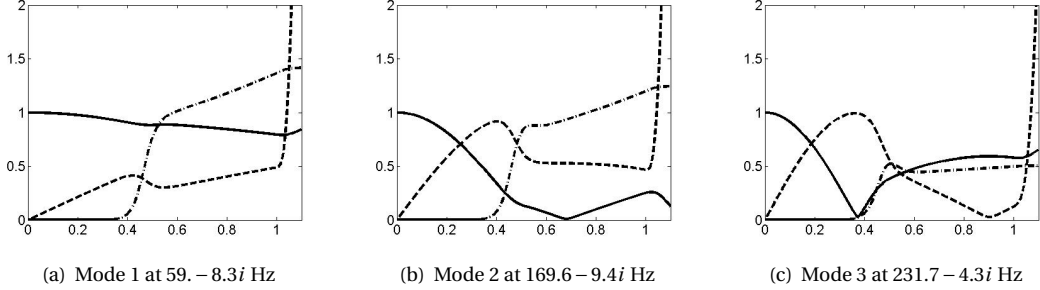


Figure 3: The first 3 modes in the configuration of Fig. 1. — : $|\hat{p}(x)|$; --- : $|\hat{u}(x)|$; - · - : $|\hat{s}(x)|$.
The fluctuating quantities are scaled by γp_0 , c_0 and $10 \times C_v$ respectively.

3.2 Transient Energy Growth & Optimal Initial Perturbation

Based on the first six eigenmodes obtained from solving the Linearized Euler Equations, the optimal initial perturbation and the transient energy growth that it may cause are then determined. These quantities are calculated using the two approaches introduced in section 2, i.e. the transient energy growth based on the classical acoustic energy $G_{ac}^m(t)$ as noted in Eq. (23), and the transient energy growth based on the total disturbance energy $G_{tot}^m(t)$ as in Eq. (30).

As the configuration allows for the presence of entropy fluctuations, the optimal initial perturbation may include acoustic and entropy fluctuations in both cases (see Fig. 5). The difference between $G_{ac}^m(t)$ and $G_{tot}^m(t)$ consists in the fact that the contribution of entropy fluctuations to the energy term are considered negligible in the former approach, whereas they are taken into account in the latter.

The temporal evolution of the terms $G_{ac}^6(t)$ and $G_{tot}^6(t)$ is shown in Fig. 4. In this plot, the time is scaled by the period of the first eigenmode which has a frequency of $f_1 = 59. - 8.3i$ Hz (cf. Fig. 3(a)); the possible transient energy growth is plotted using a log-scale.

It is obvious that the two quantities behave very differently, their maximal values being $G_{max,ac}^6 \approx 6000$ and $G_{max,tot}^6 \approx 6$. In both cases, however, the maximum possible amplification is reached at a reduced time of $t'_{max} \approx 0.5$, i.e. after half a period of the first mode. It should also be noted that the two approaches lead to similar results at very low Mach numbers, with values of $G_{max,tot}^m \approx G_{max,ac}^m \approx 1$.

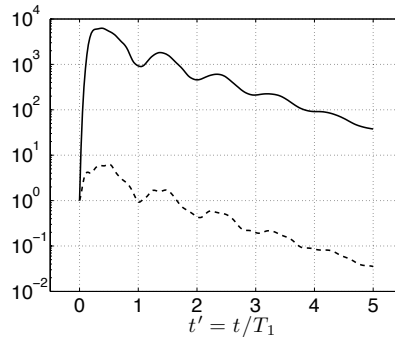


Figure 4: Temporal evolution of the maximum possible amplification as obtained from the first six eigenmodes. — $G_{ac}^6(t)$; --- $G_{tot}^6(t)$. Time is scaled by the period of the first eigenmode $t' = \frac{t}{T_1}$ with $f_1 = 59. - 8.3i$ Hz.

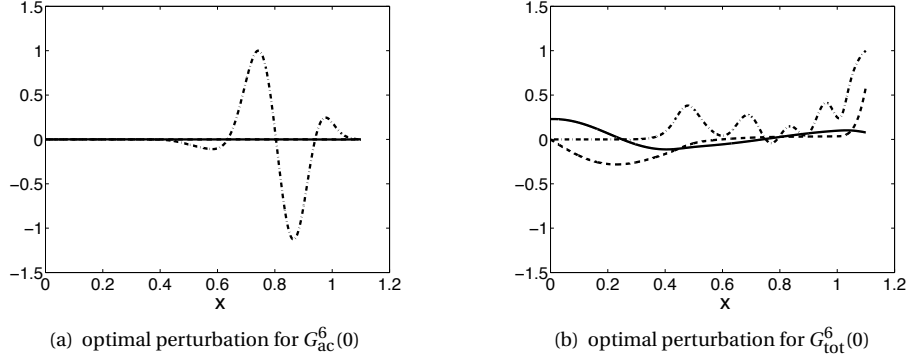


Figure 5: Spatial distribution of the optimal initial perturbation at $t = 0$: — $p'(x, t)$; --- $u'(x, t)$; -·-·- $s'(x, t)$. The fluctuating quantities are scaled by γp_0 , c_0 and C_v respectively.

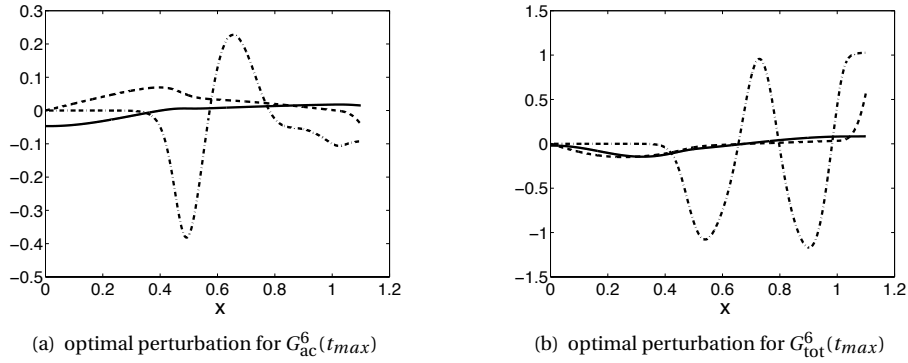


Figure 6: Spatial distribution of the optimal perturbation at $t = t_{max}$. — $p'(x, t)$; --- $u'(x, t)$; -·-·- $s'(x, t)$. The fluctuating quantities are scaled by γp_0 , c_0 and C_v respectively.

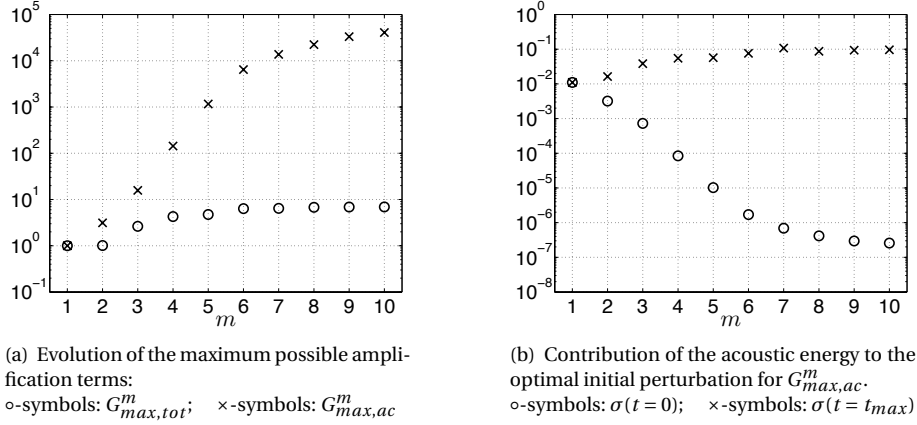
The optimal initial perturbations that allow to obtain the maximum possible amplifications $G_{ac}^6(t)$ and $G_{tot}^6(t)$ are shown in Fig. 5 for $t = 0$. Figure 6 shows the same perturbations at the moment of maximum possible amplification, i.e. at $t = t_{max}$.

In the optimal initial perturbation obtained using the total energy approach (see Fig. 5(b)), fluctuations of entropy, pressure and velocity are equally present. At the time of maximum growth $t = t_{max}$, the entropy contribution to the disturbance energy term E_{tot} has increased significantly, although the acoustic mode persists (see Fig. 6(b)). The situation is rather different for the optimal perturbation computed based on the acoustic energy only. At the initial time, the optimal perturbation contains mainly entropy fluctuations, the acoustic contribution being virtually zero (see Fig. 5(a)). However, at $t = t_{max}$ the entropy fluctuations have decreased, while the acoustic part has increased significantly (see Fig. 6(a)). This means that energy has been transferred from entropy towards acoustic fluctuations. However, as entropy fluctuations were not taken into account in the computation of the energy term, this also means that energy term E_{ac} appears to be enormously amplified as it passes from an initial value close to zero to a non-zero value at $t = t_{max}$.

This observation is consistent with the fact that a large value of $G_{max,ac}^6$ is observed in Fig. 4, while the value of $G_{max,tot}^6$ is a lot smaller.

To better understand the physical background of the difference between $G_{max,ac}^m$ and $G_{max,tot}^m$, the convergence of these quantities with respect to the number of eigenmodes m used for the analysis is displayed in Fig. 7.

From Fig. 7(a) one may conclude that the maximum transient amplification is well predicted with only 5-6 modes, when the total energy of the disturbances is considered. Adding more modes to the analysis


 Figure 7: Convergence in terms of the number of eigenmodes m used for the analysis.

does not have a huge impact on the result for $G_{max,tot}^m$. By contrast, for the growth rate based on the acoustic energy $G_{max,ac}^m$ convergence is hardly reached when 10 modes are used. It seems as if the values of $G_{max,ac}^m$ can still increase for larger numbers of eigenmodes.

This observation is confirmed by Fig. 7(b), which shows the contribution of acoustic fluctuations to the optimal initial perturbation for computations based on the acoustic energy (cf. Figs. 5(a) and 6(a)). For this plot, the value $\sigma(t)$ has been defined as the ratio of acoustic energy to total disturbance energy:

$$\sigma(t) = \frac{E_{ac}(t)}{E_{tot}(t)}, \quad (32)$$

where $E_{ac}(t)$ and $E_{tot}(t)$ are the terms defined in Eq. (13) and (28) respectively. Values of $\sigma(t)$ close to one indicate hence preponderance of acoustic fluctuations and negligible influence of entropy fluctuations, while values of $\sigma(t)$ near zero denote huge contributions of entropy fluctuations in the signal.

For the optimal perturbation corresponding to $G_{max,ac}^m$ at $t=0$, the contribution of the acoustic energy to the total energy clearly tends to zero for increasing m (o-symbols). At the same time, the contribution of acoustic energy to the perturbation at $t=t_{max}$ remains of the same order of magnitude (x-symbols). The acoustic transient growth $G_{ac}^m(t) = \max E_{ac}(t)/E_{ac}(0)$ is hence virtually unlimited for increasing values of m , as $E_{ac}(t_{max})$ does not decrease in the same way as $E_{ac}(0)$.

This behaviour is possible since the entropy mode of fluctuations can feed the acoustic mode when the mean flow is accelerated [14]. Another path from entropy to acoustic was discussed by Nicoud and Poinot [18] in the case where the thermal diffusivity is not zero. The very large value of $G_{max,ac}^6$ displayed in Fig. 4 is just and only the consequence of these physical phenomena. In other words, non-normality effects cannot be characterized by the acoustic transient growth when either mean flow or thermal diffusivity are present; the total transient growth based on the complete energy of the fluctuations should be used instead.

4 Conclusion

This article evaluates non-normal effects for a system that contains both a source of entropy fluctuations and a zone of accelerated mean flow. Rather than using a singular value decomposition approach, the determination of the maximum transient energy growth and the corresponding initial perturbation are based on an expansion in eigenmodes. These modes are obtained by solving the Linearized Euler Equations using a finite volume technique, a method that allows to take into account mean flow effects and is at the same time suitable for complex geometries.

It is shown that the eigenmodes of thermo-acoustic configurations are in general not orthogonal, which allows for a transient growth of disturbance energy. However, it is pointed out that for the analysis of

non-normal effects of such a configuration the proper choice of the energy term is crucial. Two approaches are presented in this paper, the first one being based on an energy term that is equivalent to the classic acoustic energy; the second one being based on the total disturbance energy and therefore including the contribution of entropy fluctuations. It is shown that the use of the acoustic energy concept may cause misleading results in configurations that include mean flow effects: When the energy of entropy fluctuations is neglected in the analysis, any energy transfer from entropy to acoustic fluctuations will lead to unrealistic values for transient (acoustic) energy growth.

For the presented configuration, a linear combination of five to six eigenmodes is sufficient to determine the maximum possible amplification and the optimal initial perturbation. A maximum possible amplification of $G_{max,tot}^6 \approx 6$ is found for a case with a moderate mean flow speed and where unsteady heat release is not taken into account.

Acknowledgments

KW and CS are grateful to the European Community for funding their PhD and PostDoc work under the projects AETHER (Contract No. FP6 - MRTN-CT-2006-035713) and MyPLANET (Contract No. FP7-PEOPLE - 2007-1-1-ITN -210781), respectively. This work was also performed in the framework of the project MICCA funded by the Agence Nationale pour la Recherche (Contract No. ANR-08-BLAN-0027-01).

References

- [1] K. Balasubramanian and R. I. Sujith. Non-normality and nonlinearity in combustion acoustic interaction in diffusion flames. *J. Fluid Mech.*, 594:29–57, 2008.
- [2] K. Balasubramanian and R. I. Sujith. Thermoacoustic instability in a rijke tube: Non-normality and nonlinearity. *Phys. Fluids*, 20:044103–1–11, 2008.
- [3] L. Crocco. Aspects of combustion instability in liquid propellant rocket motors. part i. *J. American Rocket Society*, 21:163–178, 1951.
- [4] L. Crocco. Aspects of combustion instability in liquid propellant rocket motors. part ii. *J. American Rocket Society*, 22:7–16, 1952.
- [5] F. E. C. Culick. Combustion instabilities in liquid-fueled propulsion systems- an overview. In *AGARD 72B PEP meeting*, 1987.
- [6] A. P. Dowling. The calculation of thermoacoustic oscillations. *J. Sound Vib.*, 180(4):557–581, 1995.
- [7] T. Gebhardt and S. Grossmann. Chaos transition despite linear stability. *Physical Review E*, 50(5):3705–3714, 1994.
- [8] A. Giauque, T. Poinot, M. Brear, and F. Nicoud. Budget of disturbance energy in gaseous reacting flows. In *Proc. of the Summer Program*, pages 285–297. Center for Turbulence Research, NASA Ames/Stanford Univ., 2006.
- [9] E. Gullaud, S. Mendez, C. Sensiau, F. Nicoud, and T. Poinot. Effect of multiperforated plates on the acoustic modes in combustors. *C. R. Acad. Sci.Mécanique*, 337(6-7):406–414, 2009.
- [10] N. Karimi, M. Brear, and W. Moase. Acoustic and disturbance energy analysis of a flow with heat communication. *J. Fluid Mech.*, 597:67–89, 2008.
- [11] H. J. Landau. On szegő's eigenvalue distribution theorem and non-hermitian kernels. *J. Analyse Math.*, 28:335–357, 1975.

- [12] T. Lieuwen and V. Yang. Combustion instabilities in gas turbine engines. operational experience, fundamental mechanisms and modeling. In *Prog. in Astronautics and Aeronautics AIAA*, volume 210, 2005.
- [13] J. Lim and J. Kim. A singular value analysis of boundary layer control. *Phys. Fluids*, 16(6), 2004.
- [14] F. E. Marble and S. Candel. Acoustic disturbances from gas nonuniformities convected through a nozzle. *J. Sound Vib.*, 55:225–243, 1977.
- [15] M. K. Myers. Transport of energy by disturbances in arbitrary steady flows. *J. Fluid Mech.*, 226:383–400, 1991.
- [16] S. Nagaraja, K. Kedia, and R. I. Sujith. Characterizing energy growth during combustion instabilities: Singular values or eigenvalues? *Proceedings of the Combustion Institute*, 32(2):2933–2940, 2009.
- [17] F. Nicoud, L. Benoit, C. Sensiau, and T. Poinso. Acoustic modes in combustors with complex impedances and multidimensional active flames. *AIAA Journal*, 45:426–441, 2007.
- [18] F. Nicoud and T. Poinso. Thermoacoustic instabilities: should the rayleigh criterion be extended to include entropy changes? *Combust. Flame*, 142:153–159, 2005.
- [19] F. Nicoud and K. Wieczorek. About the zero mach number assumption in the calculation of thermoacoustic instability. *International Journal of Spray and Combustion Dynamic*, 1:67–112, 2009.
- [20] N. Noiray, D. Durox and T. Schuller, and S. Candel. A unified framework for nonlinear combustion instability analysis based on the flame describing function a unified framework for nonlinear combustion instability analysis based on the flame describing function. *J. Fluid Mech.*, 615:139–167, 2008.
- [21] T. Poinso and D. Veynante. *Theoretical and Numerical Combustion*. R.T. Edwards, 2nd edition, 2005.
- [22] P. J. Schmid and D. S. Henningson. *Stability and Transition in Shear Flows*. Springer, New York, 2001.
- [23] F. Selimefendigil, R. I. Sujith, and W. Polifke. Identification of heat transfer dynamics for non-modal analysis of thermoacoustic stability. *Applied Mathematics and Computation*, under consideration, 2009.
- [24] C. Sensiau, F. Nicoud, and T. Poinso. A tool to study azimuthal and spinning modes in annular combustors. *Int. Journal Aeroacoustics*, 8(1):57–68, 2009.
- [25] L. N. Trefethen. Computation of pseudospectra. *Acta Numerica*, pages 247–295, 1999.
- [26] L. N. Trefethen, A. E. Trefethen, S. C. Reddy, and T. A. Driscoll. Hydrodynamic stability without eigenvalues. *Science*, 261:578–584, 1993.